# Micropulse water vapor differential absorption lidar: transmitter design and performance

**Amin R. Nehrir,[1,*] Kevin S. Repasky,[1] John L. Carlsten[2]**

[1]*Montana State University, Electrical and Computer Engineering Department, Bozeman, Montana 59715, USA*
[2]*Montana State University, Physics Department, Bozeman, Montana 59717, USA*
**amin.r.nehrir@nasa.gov*

**Abstract:** An all diode-laser-based micropulse differential absorption lidar (DIAL) laser transmitter for tropospheric water vapor and aerosol profiling is presented. The micropulse DIAL (MPD) transmitter utilizes two continuous wave (cw) external cavity diode lasers (ECDL) to seed an actively pulsed, overdriven tapered semiconductor optical amplifier (TSOA). The MPD laser produces up to 7 watts of peak power over a 1 μs pulse duration (7 μJ) and a 10 kHz pulse repetition frequency. Spectral switching between the online and offline seed lasers is achieved on a 1Hz basis using a fiber optic switch to allow for more accurate sampling of the atmospheric volume between the online and offline laser shots. The high laser spectral purity of greater than 0.9996 coupled with the broad tunability of the laser transmitter will allow for accurate measurements of tropospheric water vapor in a wide range of geographic locations under varying atmospheric conditions. This paper describes the design and performance characteristics of a third generation MPD laser transmitter with enhanced laser performance over the previous generation DIAL system.



**OCIS codes:** (140.2020) Diode lasers; (140.5960) Semiconductor lasers; (140.4480) Optical amplifiers; (120.0280) Remote sensing and sensors; (010.3640) Lidar; (280.1910) DIAL, differential absorption lidar.

## References and links

1. K. E. Trenberth, P. D. Jones, P. Ambenje, R. Bojariu, and D. Easterling, A Klein Tank, D. Parker, F. Rahimzadeh, J A Renwick, M. Rusticucci, B. Soden, and P. Zhai, "Observations: Surface and Atmospheric Climate Change. In: Climate change 2007: The physical Science Basis," Contributions of Working Group to the Fourth Assesment Report of the Intergrovernmental Panel on Climate Change (2007).
2. E. V. Browell, S. Ismail, and B. E. Grossmann, "Temperature sensitivity of differential absorption lidar measurements of water vapor in the 720-nm region," Appl. Opt. **30**(12), 1517–1524 (1991).
3. J. Bösenberg, "Ground-based differential absorption lidar for water-vapor and temperature profiling: methodology," Appl. Opt. **37**(18), 3845–3860 (1998).
4. V. Wulfmeyer and C. Walther, "Future performance of ground-based and airborne water-vapor differential absorption lidar. I. Overview and theory," Appl. Opt. **40**(30), 5304–5320 (2001).
5. A. S. Moore, K. E. Brown, W. M. Hall, J. C. Barnes, W. C. Edwards, L. B. Petway, A. D. Little, W. S. Luck, I. W. Jones, C. W. Antill, E. V. Browell, and S. Ismail, "Development of the Lidar Atmospheric Sensing Experiment (LASE) - An Advanced Airborne DIAL Instrument, " in Int. Laser Radar Conference, 281–288 (1996).
6. E. V. Browell, S. Ismail, and W. B. Grant, "Differential absorption lidar (DIAL) measurements from air and space," Appl. Phys. B **67**(4), 399–410 (1998).
7. N. S. Higdon, E. V. Browell, P. Ponsardin, B. E. Grossmann, C. F. Butler, T. H. Chyba, M. N. Mayo, R. J. Allen, A. W. Heuser, W. B. Grant, S. Ismail, S. D. Mayor, and A. F. Carter, "Airborne differential absorption lidar system for measurements of atmospheric water vapor and aerosols," Appl. Opt. **33**(27), 6422–6438 (1994).
8. G. Ehret, A. Fix, V. Weiss, G. Poberaj, and T. Baumert, "Diode-laser-seeded optical parametric oscillator for airborne water vapor DIAL application in the upper troposphere and lower stratosphere," Appl. Phys. B **67**(4), 427–431 (1998).

#175513 - $15.00 USD Received 5 Sep 2012; revised 15 Oct 2012; accepted 15 Oct 2012; published 18 Oct 2012

9. C. R. Prasad, V. A. Fromzel, J. S. Smucz, I. H. Hwang, and W. E. Hasselbrack, "A Diode-Pumped Cr:LiSAF Laser for UAV Based Water Vapor Differential Absorption Lidar (DIAL), " in IEEE Int. Geosci. Rem. Sens. Symposium, 1465–1467 (2000).
10. T. J. Axenson, N. P. Barnes, D. J. Reichle, and E. E. Koehler, "High-energy Q-switched 0.946-μm solid-state diode pumped laser," J. Opt. Soc. Am. B **19**(7), 1535–1538 (2002).
11. J. D. Spinhirne, "Micro Pulse Lidar," IEEE Trans. Geosci. Rem. Sens. **31**(1), 48–55 (1993).
12. L. S. Rothman, I. E. Gordon, A. Barbe, D. C. Benner, P. F. Bernath, M. Birk, V. Boudon, L. R. Brown, A. Campargue, J.-P. Champion, K. Chance, L. H. Coudert, V. Dana, V. M. Devi, S. Fally, J.-M. Flaud, R. R. Gamache, A. Goldman, D. Jacquemart, I. Kleiner, N. Lacome, W. J. Lafferty, J.-Y. Mandin, S. T. Massie, S. N. Mikhailenko, C. E. Miller, N. Moazzen-Ahmadi, O. V. Naumenko, A. V. Nikitin, J. Orphal, V. I. Perevalov, A. Perrin, A. Predoi-Cross, C. P. Rinsland, M. Rotger, M. Šimečková, M. A. H. Smith, K. Sung, S. A. Tashkun, J. Tennyson, R. A. Toth, A. C. Vandaele, and J. Vander Auwera, "The HITRAN 2008 molecular spectroscopic database," J. Quant. Spectrosc. Radiat. Transf. **110**(9-10), 533–572 (2009).
13. A. R. Nehrir, K. S. Repasky, and J. L. Carlsten, "Eye-Safe Diode-Laser-Based Micropulse Differential Absorption Lidar (DIAL) for Water Vapor Profiling in the Lower Troposphere," J. Atmos. Ocean. Technol. **28**(2), 131–147 (2011).
14. A. R. Nehrir, K. S. Repasky, J. A. Reagan, and J. L. Carlsten, "Optical Characterization of Continental and Biomass Burning Aerosols over Bozeman, Montana: A Case Study of the Aerosol Direct Effect," J. Geophys. Res. **116**(D21), D21201 (2011).
15. A. R. Nehrir, K. S. Repasky, J. L. Carlsten, M. D. Obland, and J. A. Shaw, "Water Vapor Profiling using a Widely Tunable, Amplified Diode Laser Based Differential Absorption Lidar (DIAL)," J. Atmos. Ocean. Technol. **26**(4), 733–745 (2009).
16. J. L. Machol, T. Ayers, K. T. Schwenz, K. W. Koenig, R. M. Hardesty, C. J. Senff, M. A. Krainak, J. B. Abshire, H. E. Bravo, and S. P. Sandberg, "Preliminary measurements with an automated compact differential absorption lidar for the profiling of water vapor," Appl. Opt. **43**(15), 3110–3121 (2004).
17. P. McNicholl and H. J. Metcalf, "Synchronous cavity mode and feedback wavelength scanning in dye laser oscillators with gratings," Appl. Opt. **24**(17), 2757–2761 (1985).
18. K. S. Repasky, G. W. Switzer, C. W. Smith, and J. L. Carlsten, "Laser diode facet modal reflectivity measurements," Appl. Opt. **39**(24), 4338–4344 (2000).
19. A. R. Nehrir, "Development of an Eye-Safe Diode-Laser-Based Micro-Pulse Differential Absorption Lidar (MP-DIAL) for Atmospheric Water vapor and Aerosol Studies," Ph.D. Dissertation, Montana State University, Electrical and Computer Engineering Department, Bozeman, MT (2011).
20. D. J. Bossert, G. C. Dente, and M. L. Tilton, "Filamentation in high-power tapered semiconductor amplifiers," Proc. SPIE **3001**, 63–73 (1997).

## 1. Introduction

Water vapor is the most dominant and variable green house gas in the Earth's atmosphere and plays a key role in driving long term climate change, atmospheric chemistry and transport, and high impact weather systems [1]. Accurate measurements of atmospheric water vapor using the DIAL technique requires a robust laser transmitter capable of accessing appropriate strength absorption lines shown in Fig. 1 with minimal sensitivity to changes in temperature and pressure while simultaneously operating with high spectral purity [2, 3]. Another key requirement for accurate retrievals of water vapor profiles is to achieve sufficient laser average power in order to reach satisfactory signal to noise ratios (SNR) with integration periods that fall below the typical lifetimes of tropospheric and boundary layer processes [4].

Most/many water vapor DIAL systems designed to target the aforementioned requirements in the 730-940 nm spectral bands have used solid state lasers such as Ti:Sapphire lasers [5, 6], Alexandrite lasers [7], optical parametric oscillators (OPO) [8], Cr:LiSAF lasers [9], and Nd:YAG lasers [10] to provide high energy laser radiation at the desired absorption band. Line narrowing of the various types of DIAL laser transmitters is typically achieved by injection seeding via diode lasers that are either in a distributed feedback or external cavity configuration [5, 8, 9]. DIAL systems that employ high pulse energy laser transmitters are valuable in applications that require high spatial and temporal resolution measurements such as from an aircraft or spacecraft platform. Although yielding high spectral purity and pulse energy, the practical use of solid state lasers is limited in DIAL applications that require deployment in standalone network configurations due to high maintenance and operation costs. These costs are often associated with the replacement of pump sources and gain medium, low electro-optical and optical-optical efficiencies, large optical footprints, and large nominal ocular hazard distances (NOHD) which is an important

#175513 - $15.00 USD Received 5 Sep 2012; revised 15 Oct 2012; accepted 15 Oct 2012; published 18 Oct 2012

requirement for autonomous systems. To overcome the near field ocular hazards associated with typical solid state DIAL transmitters as well as to satisfy the lower maximum permissible exposure (MPE) requirements in the visible-NIR part of the spectrum, an alternative approach known as the micropulse lidar (MPL) technique can be used [11]. The MPL technique minimizes the ocular hazard by beam expansion of the output of a high pulse repetition frequency (PRF) and low pulse energy laser transmitter ranging from 1 to 20 kHz, and 1-100 μJ, respectively. High SNR is then achieved via integration of the backscattered returns from multiple laser shots, typically in the range of 1-10 minutes. Furthermore, a small laser transmitter and receiver field of view is required for this technique to minimize the impacts of background solar radiation on the weak return signal.

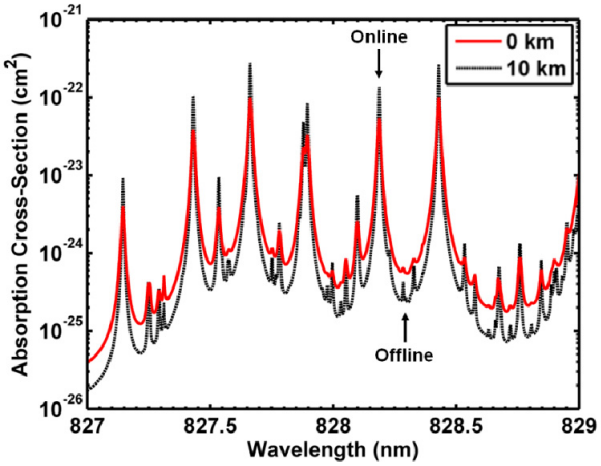


Fig. 1. Voigt profile of the water vapor absorption cross sections near the selected operating line at a 0 km (red) and 10 km (black) altitude [12]. The online and offline operating wavelengths are indicated by the arrows and are separated by 100 pm.

The MPL approach has been applied to DIAL measurements of atmospheric water vapor in the 830 nm absorption band using an all diode-laser-based transmitter and has been described in detail previously [13–16]. Most recently, a second generation MPD transmitter was developed based on a master oscillator power amplifier (MOPA) configuration where a single tunable ECDL seed laser was used to injection seed two cascaded TSOAs, yielding up to 2 watts of peak power over a 1 μs pulse duration (2 μJ) at a 20 kHz PRF [13]. Nighttime and daytime water vapor profiles were retrieved up to 4.5 km and 3 km, respectively, with integration periods approaching 20-30 minutes. This approach of a single tunable injection seeding source proved to be valuable in demonstrating the viability of the MPD technique for tropospheric measurements of water vapor, but had major limitations in the presence of rapidly changing background levels due to the slow spectral switching time between the online and offline DIAL wavelengths [13].

In this paper, we present the design and performance of a third generation MPD transmitter that will allow for higher spatial and temporal resolution profiles of tropospheric water vapor and aerosols in varying atmospheric conditions. A schematic of the third generation DIAL transmitter is shown in Fig. 2. Two custom built ECDLs stabilized to the online and offline DIAL wavelengths are used to injection seed a single stage actively pulsed TSOA operating near 830 nm via an opto-mechanical fiber optic switch. The Voigt profiles at 0 km and 10 km for the water vapor spectrum near the chosen 828.187 nm (vacuum) operating absorption line are shown in Fig. 1. The complex structure of the spectrum and interference from the neighboring lines places a stringent requirement on the laser transmitter spectral purity and frequency stability for accurate DIAL measurements in the mid-lower

#175513 - $15.00 USD Received 5 Sep 2012; revised 15 Oct 2012; accepted 15 Oct 2012; published 18 Oct 2012

troposphere. Pulsing of the MPD transmitter is achieved by actively modulating the drive current to the TSOA gain medium with a 100% modulation index square wave (1% duty cycle at a 10 kHz PRF), hence allowing for ranging of the backscattered returns. Atmospheric DIAL measurements of water vapor are then retrieved by averaging the returns from multiple laser shots (~5-10 million shots).

This paper is organized as follows. Section 2 contains a description of the ECDL design and performance. The implementation of the new fiber optic switch as well as the single stage current pulsed TSOA are presented in section 3. Finally, some brief concluding remarks are presented in section 4.

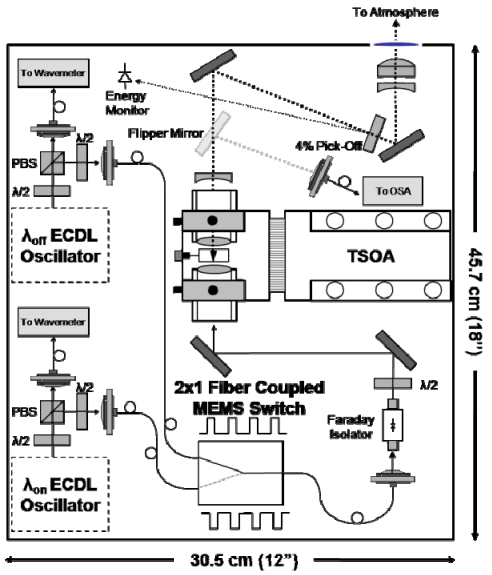


Fig. 2. Schematic of the third generation MPD transmitter. The power connections and communication lines used to drive and stabilize the seed lasers and amplifier are not presented in this illustration. The entire laser transmitter box is controlled via a laptop computer over USB and RS232 connections. The power and communication connections can be seen in a picture of the MPD transmitter box presented in Fig. 13.

## 2. Seed laser design and characterization

During the design phase of the MPD transmitter there were no spectral regions with water vapor absorption lines of appropriate strength (for tropospheric measurements) for which commercially available frequency stabilized diode lasers and TSOAs were available. The 830 nm water vapor absorption band is the only spectral region where overlap between appropriate strength water vapor absorption lines and commercially available optical amplifiers is achieved. Due to the lack of commercially available frequency stabilized diode lasers near the 830 nm water vapor absorption band during the time of the instrument design, two custom built ECDLs in a modified Littrow configuration [17] were designed and built as the injection seeding sources for the MPD transmitter. The requirements for the water vapor absorption line selection as well the laser transmitter performance specifications needed in order to retrieve accurate tropospheric water vapor number density profiles has been studied and is described in detail in the first and second generation DIAL system publications [13, 15]. The laser performance specifications for the third generation MPD transmitter presented in Table 1 at the end of section 3.2 meets all of the criteria required for accurate retrievals of water vapor number density profiles in the lower troposphere [3].

#175513 - $15.00 USD Received 5 Sep 2012; revised 15 Oct 2012; accepted 15 Oct 2012; published 18 Oct 2012

*2.1 Modified littrow ECDL design*

A schematic showing the conceptual design and a rendered image of the Solid Works model showing the major components of the ECDL are shown in Fig. 3(a) and Fig. 3(b), respectively. The spectrally broad output from the antireflection (AR) coated front facet of a 100 mW C-mounted laser diode is collimated using an 8 mm 0.5 numerical aperture (NA) aspheric lens. The collimated output is next incident on a 2100 lines/mm holographic diffraction grating (Spectragon) which spatially separates the spectral components of the laser diode. The 1st order spectral component from the diffraction grating is fed directly back into the front facet of the laser diode, providing enhanced gain at this wavelength and thereby causing the laser cavity to operate with a single longitudinal mode. The laser cavity is formed between the diffraction grating and the uncoated back facet of the laser diode chip resulting in an effective optical path length of 17 mm. Tuning of the ECDL wavelength is achieved by rotating the diffraction grating around a calculated mechanical pivot point which provides synchronous feedback to the laser from the diffraction grating at a different wavelength [17]. Typically, Littrow configured ECDLs use the 1st order diffraction from a grating to provide feedback to the laser where the specular 0th order reflection is used as the laser output. These types of ECDLs typically exhibit 5-15 mW of cw output power. A C-mounted diode laser was used in these Littrow configured ECDLs in order to reduce the 1st order loss beam that typically circulates within the classical Littrow configured ECDL cavity. By utilizing a diffraction grating that is highly efficient in the 1st order diffraction (> 90%), the output power of the ECDL is significantly increased to ~35-50 mW.

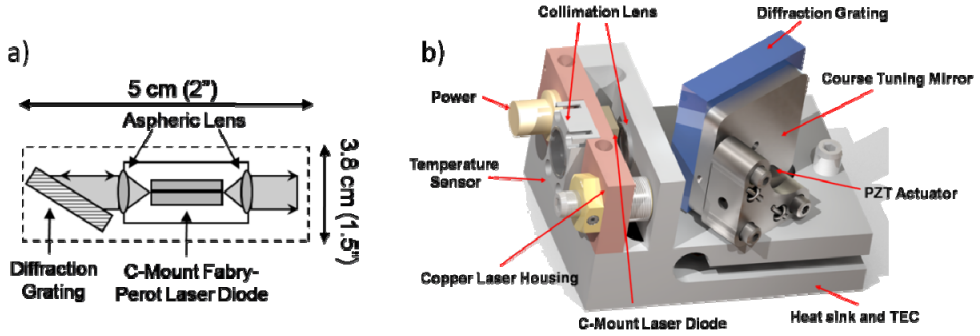


Fig. 3. (a) Schematic of the modified littrow configured ECDL. (b) Rendered image of the Solid Works drawing of the ECDL showing the major components.

The 30x30x6 mm diffraction grating used to provide feedback to the laser diode is fastened to a miniature 3 axis mirror mount (New Focus 9873-K) using UV cured epoxy. Feedback to the laser diode is optimized by making small adjustments to the three #6-80 adjustment screws on the mirror mount. Course adjustment to the ECDL output wavelength is achieved by changing the angle of the grating/mirror mount with respect to the laser diode. Fine frequency tuning of the ECDL wavelength over the free spectral range (FSR) of the external cavity is achieved by applying a voltage to the piezo electric transducer (PZT) placed between the back of the mirror housing and the same hex head ball driven screw used for coarse adjustment. The ECDL cavity is stabilized to within 0.1 °C using a thermoelectric cooler (TEC) where temperature feedback is provided using a 10 kΩ thermistor placed directly under the diode laser within the copper housing. The ECDL output is taken from the back facet of the uncoated C-mount laser diode where a 6.24 mm focal length 0.4 NA aspheric lens is used to collimate the ECDL output to a nominal beam waist diameter of 2.5 mm measured ~5 m behind the laser. The second ECDL built as the offline wavelength seeder is identical to the one described here.

#175513 - $15.00 USD Received 5 Sep 2012; revised 15 Oct 2012; accepted 15 Oct 2012; published 18 Oct 2012

*2.2 ECDL characterization*

High laser transmitter spectral purity greater than 0.995 is required for accurate DIAL measurements of atmospheric water vapor throughout the troposphere [3]. The wavelength spectra for the online and offline ECDLs captured using a 26 GHz resolution optical spectrum analyzer (Agilent 86142B) are shown in Fig. 4. Narrowing of the laser linewidth was observed for both of the seeded ECDLs (blue spectra) relative to the emitted broadband amplified spontaneous emission (ASE) spectrum when the feedback to the laser diode (red spectra) was removed. Side mode suppression ratios (SMSR) exceeding 45 dBm were measured for both ECDLs indicating high spectral purity for the water vapor DIAL measurement.

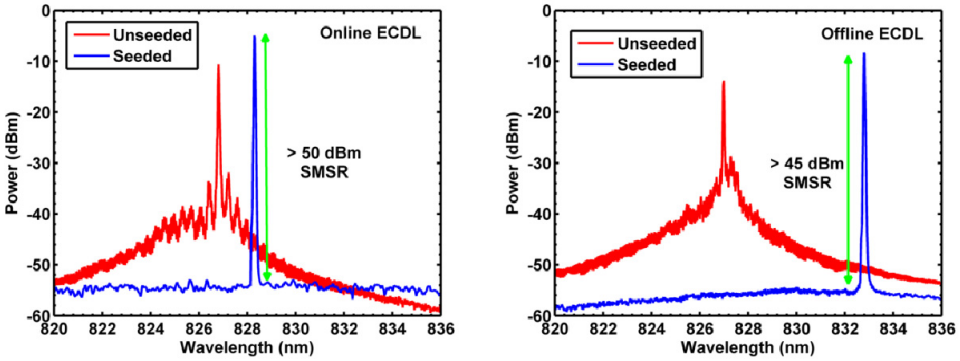


Fig. 4. Wavelength spectra of the seeded and unseeded online (left) and offline (right) ECDLs. Narrowing of the laser linewidth is observed in each case when the ECDL has sufficient feedback from a diffraction grating. The ASE in both ECDLs are suppressed to greater than 45 dBm below the peak of the seeded spectrum.

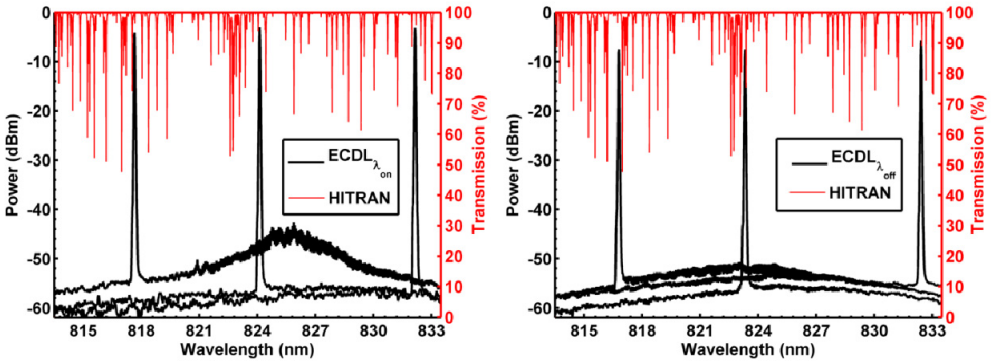


Fig. 5. Wavelength tuning spectrum for the online (left) and offline (right) ECDLs. Water vapor absorption lines accessible within the coarse tuning range of the ECDLs are also plotted on the right vertical axis using a HITRAN simulation over a 1 km horizontal path length [12].

The broad tunability of the ECDLs gives access to many variable strength water vapor absorption lines in the 830 nm spectral region, allowing for operation in varying atmospheric conditions and geographic locations. A coarse tuning range of the online and offline ECDLs in addition to the accessible water vapor absorption lines within the ECDL tuning ranges are shown in Fig. 5. The coarse tuning range exceeding 15 nm is achievable in both lasers while maintaining single longitudinal mode operation.

The primary motivation for using the modified Littrow ECDL in the third generation DIAL transmitter was to achieve higher seed laser output power while maintaining good laser

#175513 - $15.00 USD Received 5 Sep 2012; revised 15 Oct 2012; accepted 15 Oct 2012; published 18 Oct 2012

spectral properties in order to alleviate the need for a cascaded amplification stage as used in the second generation DIAL transmitter [13]. Typical ECDLs have an intracavity loss beam from the 1st order diffraction off of the grating, hence limiting the output power available via the specular 0th order reflection to ~5-15 mW. The modified Littrow ECDLs here have no loss beam where the 1st order diffracted light is sent directly back into the laser diode, producing output powers at the back facet of the laser diode ranging between 35 and 50 mW. The intracavity power circulating between the diffraction grating and the back facet of the laser diode is estimated to be approximately 60 mW. Figure 6 shows the power vs current (PI) curves for the two ECDLs where the output wavelength is also presented as the false color at each data point and shows the current tuning characteristics of the ECDLs. Lasing thresholds of 56 mA and 38 mA can be seen for the online and offline ECDLs, respectively. A maximum output power of ~35 mW was achieved for a fixed grating position for the two seed lasers. The wavelength current tuning measured using a ± 55 MHZ resolution Burleigh Wavemeter results from the increase in the laser diode charge carrier density within the gain medium which effectively increases the index of refraction and effective optical path length. The tuning continues with increasing current until a mode hop occurs [18].

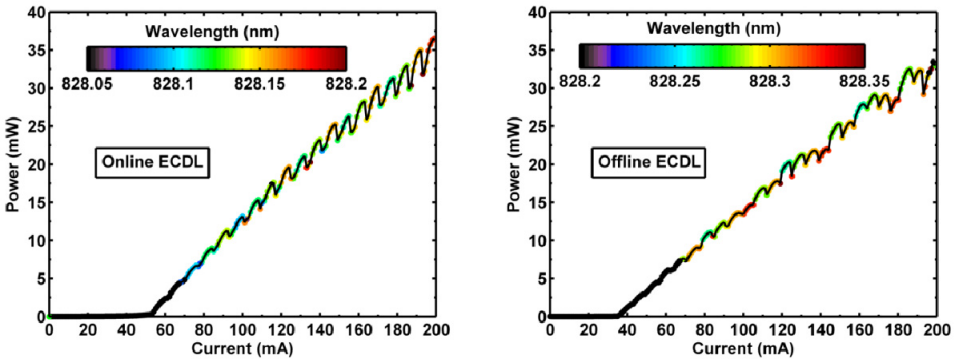


Fig. 6. PI curves for the online (left) and offline (right) ECDLs. The output wavelength is plotted as the color at each data point and shows the wavelength tuning characteristics and mode hopping as the forward current is increased.

Accurate measurements of atmospheric water vapor using the DIAL technique require good laser spectral properties [3]. The laser linewidth of the two ECDLs were inferred by measuring the half width of the heterodyne beat note between the two seed sources. The width of the heterodyne beat note is proportional to the spectral width of each ECDL and was measured using a 40 GHz photodetector (New Focus) and a 21 GHz radio frequency (RF) spectrum analyzer. The measured heterodyne spectra from the two seed sources is shown in Fig. 7. An 852 kHz 3dB bandwidth around the central peak of the beat note signal was measured using a 100 kHz resolution bandwidth and a ~1 ms sweep time. Assuming the spectral properties of the two lasers are similar, the linewidth of the each ECDL is then estimated to contribute to half of the FWHM width of the measured heterodyne signal, yielding a 426 kHz FWHM linewidth for each seed laser. The measured laser linewidths are well below the 390 MHz linewidth required for accurate measurements of water vapor [3]. The narrow laser linewidths allow for high spectral resolution tuning along the ~6 GHz pressure broadened width (FWHM) of the water vapor absorption line. The sidebands observed on the heterodyne spectra result from optical feedback to ECDLs from the fiber based beam splitter/combiner. Although clearly noticeable, the feedback from the fiber splitter/combiner is ~50-70 dB below the peak of the ECDL heterodyne signal and is considered to be negligible to the overall laser linewidth measurement.

#175513 - $15.00 USD Received 5 Sep 2012; revised 15 Oct 2012; accepted 15 Oct 2012; published 18 Oct 2012

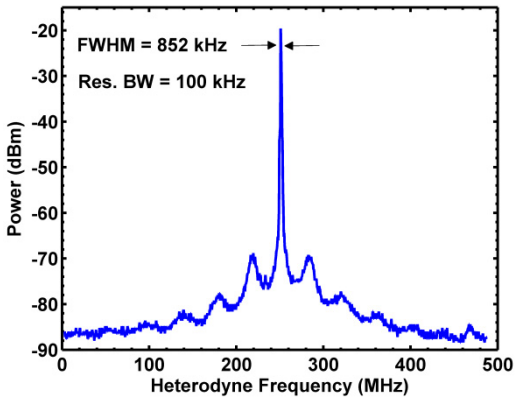


Fig. 7. Measured heterodyne beat note from two similar modified Littrow ECDLs. The online ECDL was locked to the center of the 828.187 nm water vapor absorption line using a wavemeter while the offline seed laser was tuned and locked ~250 MHz away using a second wavemeter.

Fine tuning of the ECDL wavelength is achieved via small adjustments to the diffraction grating angle using a PZT. A typical online ECDL frequency tuning curve normalized to the center frequency of the chosen 828.187 nm water vapor absorption line is shown in Fig. 8(a). Continuous tuning of the ECDL as a function of the applied voltage to the PZT is seen over the 6.45 GHz FSR of the external cavity. With a manufacturer specified maximum bias voltage of 120 V applied to the PZT, continuous tuning of the ECDL over the ~6 GHz FWHM pressure broadened water vapor absorption line can be achieved, allowing for sideline tuning in order to decrease the water vapor optical depth for operation in high moisture conditions. Approximately 5-6 GHz of sideline tuning is required to decrease the absorption cross section by an order of magnitude. Locking of the online ECDL to a given spectral position along a water vapor absorption line is achieved by means of feedback from a Burleigh WA-1500 wavemeter to the diffraction grating PZT using the LabView programming environment [13, 15]. A variable attenuator consisting of a half waveplate and a polarizing beam splitting cube (PBS) is used to pick off a small fraction of the seed laser light which is then fiber coupled and delivered to the wavemeter for frequency locking to the absorption line. The wavemeter reading is polled at up to a 2 Hz sampling rate where a correction voltage is applied to the ECDL PZT via electronic feedback through LabView in order lock to any spectral position along a selected water vapor absorption feature to within ± 55 MHz. This meets the ± 210 MHz frequency stability requirement needed for accurate measurements of tropospheric water vapor in the 720 nm spectral band [3] where the absorption line shapes are comparable to those in the 830 nm spectral band, however tighter requirements are needed in the upper troppshere where the absorption lineshape is much narrower due to the absence of pressure broadening. Tropospheric water vapor profiling using sideline tuning has been previously reported using this technique where the Voigt profile was used to estimate the absorption line shape as a function of altitude [13]. To minimize the effects of laser frequency jitter on the uncertainty in the absorption cross section, future efforts to stabilize the laser wavelength to the water vapor absorption line will use frequency modulation spectroscopy through a multipath gas absorption cell to increase the frequency stability to better than ± 5 MHz [5].

Figure 8(b) shows the frequency locking response of the online ECDL to the center of the water vapor absorption line using the wavemeter to provide feedback to the grating PZT over a 120 minute time period. Locking of the ECDL to the absorption line was engaged 60 minutes after the start of the measurement. The ECDL was allowed to drift prior to engaging the wavelength stabilization to demonstrate the sensitivity of the laser cavity to abrupt and

#175513 - $15.00 USD Received 5 Sep 2012; revised 15 Oct 2012; accepted 15 Oct 2012; published 18 Oct 2012

drastic changes in temperature and pressure. A heat gun was placed near the ECDL 45 minutes after the start of the measurement to assess the resilience of the cavity to anomalous fluctuations in the temperature. A large swing in the external cavity frequency can be seen where after several minutes, the cavity recovered from the large frequency shift. Stable operation of the locked ECDL can be seen for the subsequent 120 minutes after the locking was engaged. Continuous locking of the online ECDL has been observed for over a 24 hour period during instrument operation where a large temperature gradient between the outside air and the lidar laboratory in the early morning causes a mode hop in the ECDLs.

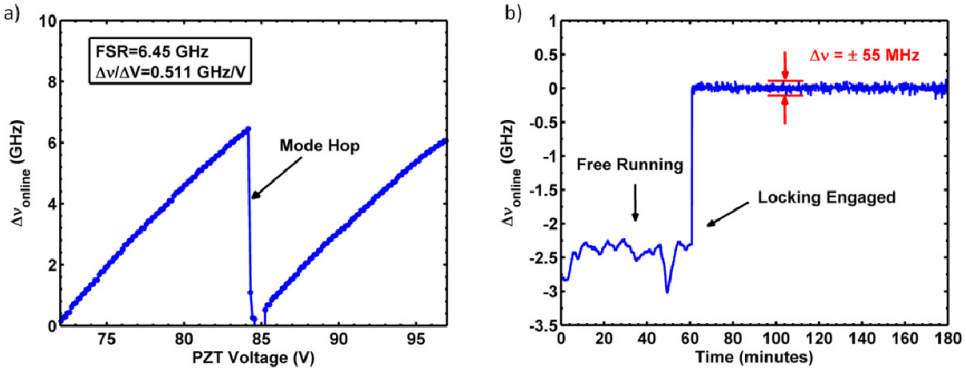


Fig. 8. (a) Fine tuning response of the modified Littrow ECDL. Continuous tuning is observed over the 6.45 GHZ FSR of the external cavity until a mode hope occurs. (b) Measured response of the online ECDL output frequency before and after the labview locking loop was engaged to stabilize the laser to the center of the 828.187 nm water vapor absorption line. The software controlled locking loop was engaged 60 minutes after the start of the measurement.

## 3. Tapered amplifier and optical switch characterization

### *3.1 Optical switch*

The seed lasers described above have good spectral properties but have low cw output power. The output of the two ECDLs are amplified using a single stage current pulsed TSOA. To minimize the effects of atmospheric changes in the backscattered returns between the DIAL online and offline wavelengths, a fiber optic switch is used to sequentially deliver light from one of the two seed lasers to the pulsed TSOA with a 1Hz switching frequency. Seed laser light rejected from the PBS cubes are fiber coupled into the two legs of a 2x1 polarization maintaining (PM) electromechanical fiber optic switch (Agiltron LB Series 2x1 PM Switch). The three ports of the optical switch (as well as the beamsplitter used for linewidth measurement) have angled physical contact (APC) fiber connectors which minimizes feedback to the seed laser source and alleviates the need for optical isolators and increases the transmitter optical throughput. The use of a PM optical switch maintains the high polarization ratio of the two seed lasers which are > 100:1 and allows for efficient seeding of the polarization sensitive TSOA. Furthermore, the optical cross talk between the two channels of the switch measured using an optical spectrum analyzer is below 80 dB, which is the sensitivity level of the spectrometer used to make the measurement. This ensures little to no cross talk between the online and offline seed lasers and allows for high spectral purity of the transmitted output at both the online and offline wavelengths. The polarization of the two seed lasers is aligned to the fast axis of the PM fibers using a second half wave plate place directly before the fiber coupler.

The switch is a non-latching device which acts as a shutter for one of the two ports when the electrical power is either applied or removed. A nanosecond rise time detector was used to measure the switching performance of the fiber optic switch. The time resolved switching behavior of the device for each channel is shown in Fig. 9. The switching time (90%) between

#175513 - $15.00 USD Received 5 Sep 2012; revised 15 Oct 2012; accepted 15 Oct 2012; published 18 Oct 2012

the two ECDLs was measured to be ~1 ms, resulting in the loss of 10 laser shots during each switching event given a 10 kHz PRF. This relatively short dead time ensures that the backward propagating ASE within the pulsed TSOA does not have sufficient time to grow and damage the input facet of the amplifier. After the optical switch, the output is sent through a 30 dB optical isolator to prevent unwanted feedback from the amplifier's ASE to the seed lasers. A half wave plate is then used to align the polarization of the seed source perpendicular to the TSOA junction plane for maximum extraction of the amplifier gain.

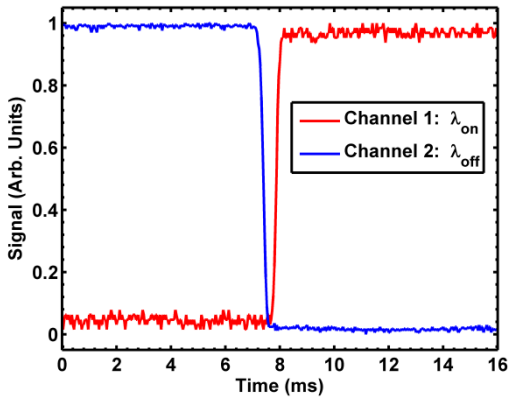


Fig. 9. Temporal switching response of the electro-mechanical fiber optic switch. Approximately 10 laser shots (0.1% of the shots at 10 kHz) are skipped during each switching event between the online and offline seed lasers.

*3.2 Tapered amplifier*

The third generation DIAL transmitter utilizes a new 4.0 mm length single stage pulsed TSOA (Eagleyard EYP-TPA-0830-01000) to amplify the cw output from the two modified littrow seed lasers. A 4.5 mm focal length aspheric lens is used to couple the seed light into the ridge waveguide section of the TSOA. The amplifier is placed in the same housing and utilizes the same pulsed current source described in the previous generation instrument paper [13]. With ~5-10 mW of seed power available at the input aperture to the TSOA, peak pulse energies exceeding 7 μJ were measured for a PRF and pulse width duration of 10 kHz and 1 μs, respectively. The decrease in the PRF of the third generation transmitter (second generation transmitter) to10 kHz (20 kHz) was to allow for a larger maximum unambiguous range of 15 km (7.5 km) as well as to allow for background subtraction at the tail end of the return pulse from the upper atmosphere. The TSOA output pulse energy as a function of the pulsed forward current for the seeded online and offline wavelengths as well as the temporal pulse shape characteristics are shown in Fig. 10(a) and Fig. 10(b), respectively.

The output pulse energy of the TSOA exhibits a linear response to the input pump current above 2.5 amps where the TSOA lasing threshold is passed. Sufficient gain in the amplifier from 2.5 to 8.0 A results in almost equal output pulse energies between the online and offline wavelengths for a 40% difference in the available seed power from the ECDLs. A calibrated time resolved capture of the TSOA output pulse power at the online and offline wavelengths for an 8.0 A maximum pulsed forward current is shown in Fig. 10(b). A low inductance flat cable is used to pump the TSOA using an internally triggered Directed Energy Incorporated PCX-7410 pulsed current source which provides a clean and repeatable pulse shape with a rise and fall time of ~30 ns and 50 ns, respectively. The 3.5-7 x increase in the output pulse energy over the second generation DIAL transmitter is a major achievement that has allowed for measurements of water vapor and aerosol profiles up to ~6 km and 15 km, respectively. The output pulse energy stability of the DIAL transmitter was measured to be less than 1-2% of the peak pulse energy over a 1 week period.

#175513 - $15.00 USD Received 5 Sep 2012; revised 15 Oct 2012; accepted 15 Oct 2012; published 18 Oct 2012

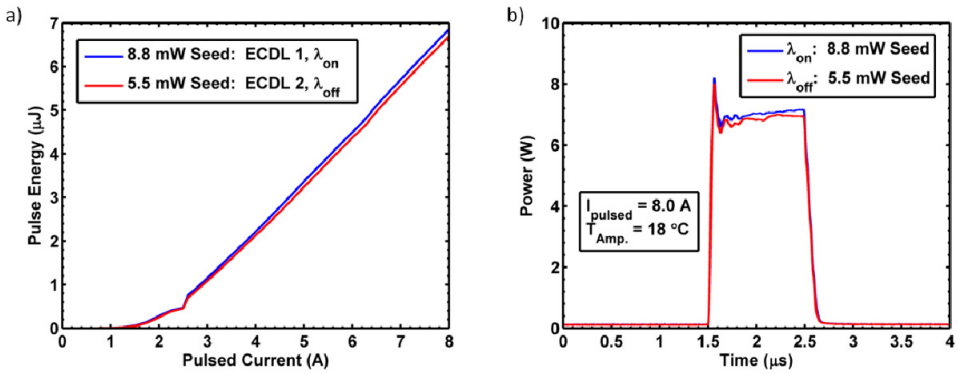


Fig. 10. (a) Output pulse energy as a function of the pulsed forward current to the TSOA for the online and offline seed lasers. The knee in the PI curve near 2.5 A represents the lasing threshold for the TSOA. (b) Time dependence of the output power of the injection seeded TSOA at the online and offline wavelengths for a 1 μs duration 8 A current pulse. The PRF for this measurement was set at 10 kHz, corresponding to a 1% duty cycle.

Recently, new 100 mW Distributed Bragg Reflector (DBR) laser diodes (Photodigm) were implemented in the DIAL transmitter to replace the ECDL seed lasers. The linewidth and SMSR of the new DBR lasers are < 2 MHz and >35 dB, respectively, which should yield similar spectral purities of the pulsed transmitter output as for the ECDL seed sources described here. The wavelength stability, when actively stabilized using the methods described above is limited to the resolution of the Burleigh wavemeter. The inclusion of the new high power seed lasers as well as a re-optimization of the TSOA coupling alignment yielded an increase in the output pulse energy exceeding 13 μJ. The pulse energy stability with the new configuration was measured to be less than 1% of the peak pulse energy over a 3 week operating period. A detailed description of the performance of the new seed lasers and their implementation in the DIAL transmitter will be presented in a future paper.

The enhanced output pulse energy of the MPD transmitter will result in an increased SNR at longer ranges from the instrument for a fixed integration period, allowing for water vapor and aerosol profiling well into the free troposphere. In the upper atmosphere where the width of the pressure broadened absorption line decreases, the accuracy of the water vapor retrievals becomes much more sensitive to the laser transmitter spectral properties, hence the preservation of the good seed laser properties through the TSOA is important. A spectrum of the unseeded and seeded DIAL transmitter at the online wavelength for a maximum pulsed operating current of 8.0 A is shown in Fig. 11. For the unseeded case, the broad gain spectrum of the TSOA can be seen. Despite a manufacturer deposited AR coating on both facets of the amplifier, lasing within the amplifier cavity can be seen at high operating currents. The injection seeded TSOA spectrum for an ~8.0 mW seed power shows good suppression of the broadband ASE while maintaining the narrow linewidth of the seed laser with a measured SMSR > 45 dBm. Sufficient gain and good injection seeding give way to exceptional laser transmitter spectral properties for high peak pulsed currents. Horizontal path hard target spectral purity measurements have indicated that the spectral purity of the pulsed laser transmitter exceeds 0.9996 at 850 mb elevation where pressure broadening is the dominant line broadening effect [19]. A more accurate representation of the laser spectral purity measurement is achieved using a long path herriott type gas absorption cell filled with low partial pressure of water vapor. This decreases the effect of pressure broadening on the absorption line and increases the sensitivity of the absorption to the laser linewidth. Future efforts to measure the transmitter spectral purity will employ this method. Lastly the high spectral purity measurements indicated that little or no frequency chirp associated with the fast rise/fall-time current pulsing of the TSOA was present.

#175513 - $15.00 USD Received 5 Sep 2012; revised 15 Oct 2012; accepted 15 Oct 2012; published 18 Oct 2012

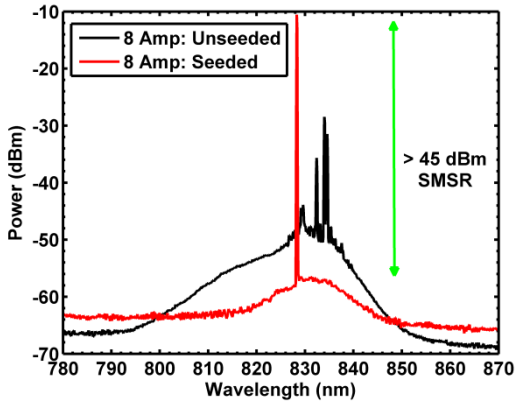


Fig. 11. Measured output spectra of the seeded and unseeded DIAL transmitter at the online wavelength using a maximum operating pulsed current of 8.0 A. Suppression of the TSOA ASE spectrum can be seen when a seed is applied to the traveling wave amplifier, yielding a SMSR > 45 dBm.

The output of the pulsed TSOA is collimated using the same two stage (aspheric lens and cylindrical lens) beam forming optics utilized in the second generation DIAL transmitter [13]. Good beam quality coupled with sufficient beam expansion is essential for aerosol and water vapor retrievals at further ranges from the DIAL instrument. The transmitted beam profile was analyzed using a charged coupled device (CCD) camera to assess the impacts of high current pulsing on the beam quality of the MPD transmitter. Figure 12(a) and Fig. 12(b) show the beam profiles of the collimated output of the TSOA for the unseeded and seeded cases, respectively. For the cw unseeded case, a manufacturer specified maximum bias current of 3.0 A was supplied to the amplifier to exaggerate the astigmatic nature of the output beam. When injection seeded, the ASE is suppressed and a nominally circular beam can be seen although filamentation within the profile is prominent. The level of the filamentation is directly proportional to the forward current and the contrast of the striations increases with increasing levels of pump to the gain medium.

Figure 12(b) shows the measured beam profile for the seeded output of the TSOA under pulsed operation (1μs pulse duration at 10 kHz PRF) for an 8 mW seed. The striations in the beam profile are more pronounced in the pulsed regime. The lack of suppression of the filamentation also shows less sensitivity to injection seeding. This filamentation behavior has previously been studied and is attributed largely to the dependence of the refractive index of the TSOA gain medium on the carrier density, i.e. the magnitude of the forward current [20]. Specifically, the striations are thought to originate from small impurities in the gain region which cause small changes in the local index/carrier density and amplifies to become more prominent as the wave propagates down the amplifier. The index induced striations are not believed to result in multimode operation of the pulsed output and do not limit the divergence of the transmitted beam. The parallel and perpendicular cross-sections of the injection seeded output from Fig. 12(b) are shown in Fig. 12(c). The striations are clearly visible in the flared parallel axis of the amplifier where the beam shape envelope nominally fits a 3.0 mm Gaussian distribution. The perpendicular axis of the TSOA output which more closely resembles the dimensions of a typical ridge waveguide single mode laser diode shows less evidence of filamentation and more closely overlaps with a Gaussian fit to a 3.0 mm output beam diameter.

#175513 - $15.00 USD Received 5 Sep 2012; revised 15 Oct 2012; accepted 15 Oct 2012; published 18 Oct 2012

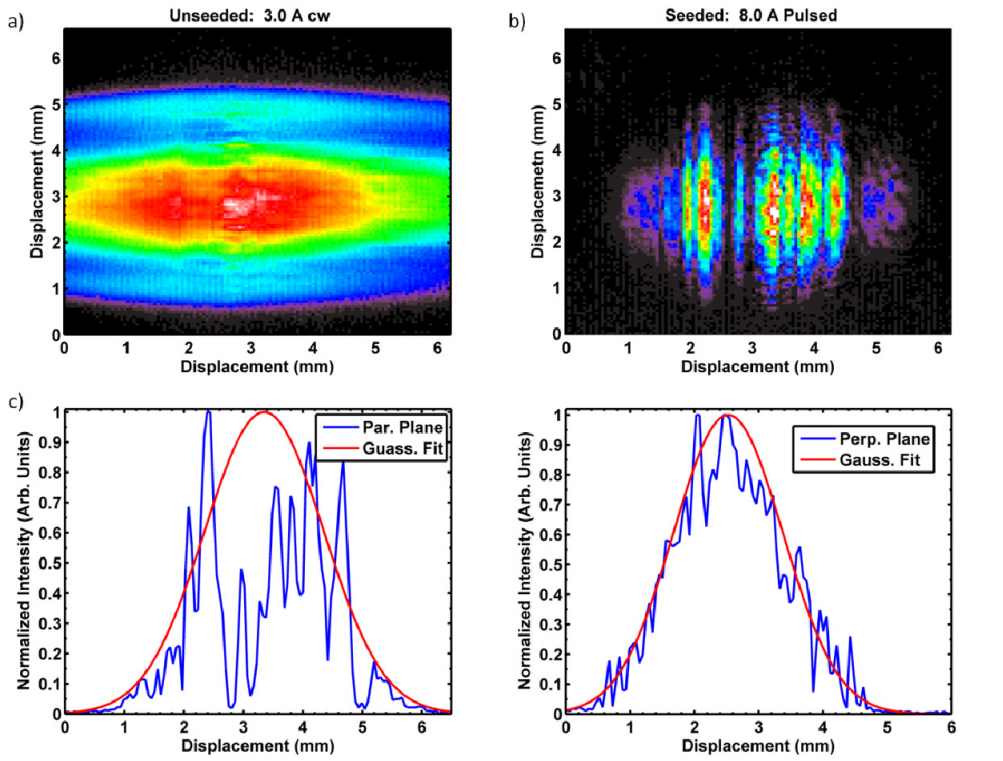


Fig. 12. (a) Beam profile for the unseeded TSOA output for a cw 3 A bias current. (b) Beam profile for the 8 A pulsed TSOA operation. Both beam profiles were optically attenuated to prevent damage to the CCD camera. (c) Parallel and perpendicular beam profile cross-sections of the injection seeded pulsed output shown in part b.

Although unattractive, the non uniform output from the TSOA does not seem to pose a significant problem for long range beam propagation as excellent return signals have been recorded at ranges exceeding 15 km with appropriate beam expansion. The MPD receiver is designed to have a field of view 1.5 times larger than the transmitter divergence to minimize the effects of atmospheric turbulence and drift in the alignment on the backscattered returns. The collimated output from the TSOA is next incident on a ~4% wedge beam sampler, shown in Fig. 2, used to direct light to an energy monitor used for power normalization of the DIAL returns. An optional flipper mirror and fiber coupler can be used for output beam spectral property diagnostics and receiver alignment. The light transmitted by the beam sampler is next incident on a 10x Galilean beam expander used to increase the beam diameter to 32 mm and decrease the divergence of the transmitted beam to ~100 μrad, and also to decrease the NOHD to 2.6 km. The output beam is finally transmitted to the atmosphere coaxially with the telescope via two 45 degree turning mirrors that are directly joined to the transmitter box.

Autonomous lidar systems operated in a network configuration such as the one proposed here require eye safety at the exit aperture of the system transmitter in order to allow for operation in a multitude of geographic locations to minimize the potential for ocular hazard to humans as well as for the need for oversight from the Federal Aviation Administration (FAA). To assure zero ocular hazard at close distances to the DIAL transmitter, the most stringent of the three laser eye safety requirements imposed by the American National Standards Institute (ANSI) must be met. The three requirements are 1) Single Pulse MPE which prevents against thermal injury from an individual pulse, 2) Average Power MPE which prevents against thermal injury from heat buildup in the retina, and 3) Multiple Pulse MPE which prevents against cumulative thermal injury from individual sub-threshold laser

#175513 - $15.00 USD Received 5 Sep 2012; revised 15 Oct 2012; accepted 15 Oct 2012; published 18 Oct 2012

pulses. By achieving eye-safety under the most stringent requirement, all three conditions are inherently satisfied. A misinterpretation of the ANSI standard presented for the second generation DIAL instrument [13] yielded an NOHD of 0-m. A reanalysis of the second generation DIAL system parameters yields an NOHD of 0.6 km. For the current configuration of the third generation DIAL transmitter (7 μJ pulse energy, 10 kHz PRF, ~100 μrad full angle divergence, 3.2 cm diameter exit beam, and 10 second direct exposure time), the latter two and more stringent of the ANSI criterions are not satisfied due to the high pulse repetition frequency, resulting in a NOHD of approximately 2.6 km above the exit aperture of the instrument.

**Table 1. Laser transmitter performance specifications**

| Parameter | Measurement |
|---|---|
| Laser Oscillator | Modified Littrow ECDL |
| Laser Amplifier | Tapered Semiconductor Optical Amplifier |
| Transmitted Wavelengths (Vacuum) | 828.187 nm (online), 828.187-828.23 nm (sideline), 828.287 nm (offline) |
| Pulse Repetition Frequency | 10 kHz |
| Pulse Length | 1 μs |
| Pulse Energy | 7 μJ |
| Short-Term Bandwidth | ≤ 0.5 MHz |
| Long-Term Bandwidth | ± 55 MHz |
| Spectral Purity | > 0.9996 |
| Beam Diameter | 32 mm |
| Beam Divergence | 100 μrad |
| NOHD | 2.6 km |
| Spectral Switching Time | 1-6 seconds |

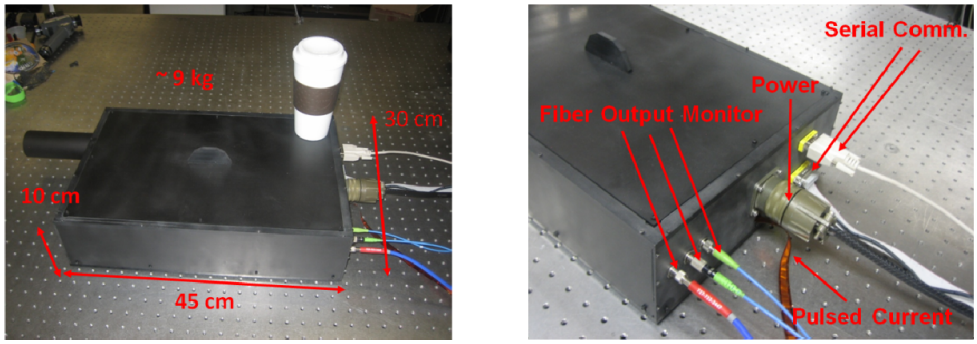


Fig. 13. Pictures of the laser transmitter box depicting the relative size of the DIAL transmitter as well as showing the various monitoring, communications, and power connections.

In order to satisfy a MPE of 51 nJ/cm$^2$ resulting from the third and most restrictive MPE criteria stated above, and thereby achieve a NOHD of 0-m for the current DIAL transmitter, a second beam expander is required. A 4.75 x beam expander was designed and built to increase the transmitted beam diameter to 15.24 cm, thereby decreasing the multiple shot MPE to 39 nJ/cm$^2$ and reducing the NOHD to 0-m. The specifications for the third generation MPD transmitter described here as well as a picture of the completed laser transmitter box (without the final beam expander) are shown in Table 1 and Fig. 13, respectively.

## 4. Conclusion

We present the design and performance of an all semiconductor-based micropulse laser transmitter, a novel and cost effective method for measuring range resolved profiles of atmospheric water vapor using the DIAL technique. Two Littrow configured cw ECDLs are used as the online and offline DIAL wavelength laser sources which are used to injection seed an overdriven current pulsed TSOA. Spectral switching between the online and offline lasers

#175513 - $15.00 USD Received 5 Sep 2012; revised 15 Oct 2012; accepted 15 Oct 2012; published 18 Oct 2012

is achieved using a 2x1 optical switch operated at a 1 Hz 50% duty cycle. The cw ECDL sources are amplified and pulsed using over driven current pulses to a temperature stabilized TSOA. Pulse energies approaching 7 μJ have been achieved using 8 A drive currents with 1 μs and 10 kHz pulse width and PRF, respectively. The factor of 60 decrease in the spectral switching time between the online and offline DIAL wavelengths compared to the previous generation DIAL transmitter has allowed for retrievals of tropospheric water vapor profiles during daytime operation as well as in the presence of rapidly changing background scenes (i.e. in between broken clouds) and heterogeneous aerosol layers [19].

The large course tuning range and high spectral purity of the diode-based MOPA laser transmitter provides flexibility in selecting appropriate strength water vapor absorption lines which are also insensitive to changes in atmospheric temperature, thereby allowing for operation in various geographic locations. With proper beam expansion the DIAL transmitter can achieve a NOHD of 0 m, thus allowing for full-time operation in any urban or suburban setting without the need for oversight from the FAA. Autonomous and full-time operating DIAL systems used for monitoring atmospheric trace gases such as water vapor can be realized in a network configuration using the low cost and compact laser transmitter described here. Future work to further enhance the performance of the diode-laser-based DIAL transmitter is aimed at increasing the output pulse energy by exploring different pulsing and injection seeding techniques; incorporating an active electronic locking system to stabilize the online and offline seed lasers to any spectral position along a given absorption feature without the need for a wavemeter; and decreasing the spectral switching time to be on the order of ~100-200 μs to more accurately sample the atmospheric volume between the online and offline laser shots. Achieving these enhancements would satisfy the stringent laser requirements needed for retrieving high spatial and temporal resolution tropospheric water vapor and aerosol profiles from both a ground-based network of instruments or an airborne platform using a single low cost automated DIAL system.

**Acknowledgments**

The authors would like to thank Dr. Paul Nachman for fruitful discussions during the design process of the transmitter seed lasers as well the spectral purity measurements. This work was supported by NASA EPSCoR under grant # NNX08AT69A and the NASA Graduate Student Researchers Program (GSRP) under grant # NNX08AR90H.

#175513 - $15.00 USD Received 5 Sep 2012; revised 15 Oct 2012; accepted 15 Oct 2012; published 18 Oct 2012